OBSERVATION OF BEAM-EXCITED DIPOLE MODES IN TRAVELING WAVE ACCELERATOR STRUCTURES*

A. M. Vetter, J. L. Adamski, W. J. Gallagher

Boeing Aerospace Co., P.O. Box 3999, Seattle, Wash. 98124

Beamline tests on a series of waveguide models have recently been completed at the Boeing Radiation Effects Laboratory. The purpose of these tests has been to study beam excitation of the dipole modes which participate in regenerative and cumulative beam breakup processes in RF linac waveguides. Cell excitation patterns, dependence on transverse beam displacement from the axis, and comparative excitation levels in waveguides of different design were measured.

Apparatus

Four brazed copper waveguide models were designed and built for these studies. Two are of the conventional disk-loaded type (Fig. 1), one having a phase shift per cell of $2\pi/3$ for the accelerating mode the other having a phase shift of $3\pi/4$. These models are 19 and 18 cells long, respectively. The other two models are of the Boeing contoured cavity design which features larger beam apertures with nose cones and rounded cell contours (Fig. 1). These two contoured cavity waveguides are 17 cells in length and are nominally identical except that one of them has eight radial slots in each iris(Fig. 2).

The cell dimensions of each of the test waveguides vary from cell to cell, modeling the appropriate taper for constant gradient operation in the accelerator mode, which is nominally at 2856 MHz. HEM_{11} mode field profiles in such guides are generally highly nonuniform. In fact, the lower frequency dipole modes are found not to propagate in the downstream end of the waveguide, but are generally confined to the first dozen or so cells.[1]

In order to explore the cell excitation pattern of beam-excited dipole modes in these waveguides, magnetic loop probes are placed in each cell. A selection of ten of these probes, distributed along the length of the waveguide, was connected by low loss coaxial cables to the experimenter's area. There a preselected spectrum analyzer (Tektronix 492P) and synthesized signal generator (Hewlett Packard 8672A) could be connected to any of the ten cables. Losses in the cables are typically 5 dB each way at 4 GHz.

The experimental layout is shown schematically in Fig. 3. After leaving the 10 MeV section of the linac and passing through a quadrupole focussing doublet, the beam enters a translator consisting of two sets of steering coils separated by a 1.5 m drift. These coils enable the operator to control both the displacement and angle of the beam as it enters the test waveguide.

On either end of the test waveguide, stripline position sensors are mounted. These determine the transverse displacement of the beam at each end of the test waveguide. After passing through the final stripline monitor, the beam is transported through a shielding wall and dumped.

*Work supported by the Boeing Aerospace Co. and DARPA/ONR under contracts N00014-82-C-0548 and N00014-85-C-0039.

Procedure

The dipole modes of interest (the TM_{11}-like modes) could be excited by either the signal generator or by the beam. Excitation by the signal generator is CW, so that the spectrum analyzer may be used with a narrow resolution bandwidth which reduces the noise floor.

Signal generator excitation is useful for frequency calibration and preselector peaking of the spectrum analyzer. It also enables the cell excitation pattern of the modes to be determined.

Excitation by the beam is limited in these experiments by the maximum beam pulse length of ~ 8μs. In fact, we found the greatest excitation when the beam pulse was as short as practical, roughly 15ns full width. This means that the 0.5μs decay time of the dipole modes determines the signal duration at the spectrum analyzer. Best signal/noise ratio is obtained with 1 MHz resolution bandwidth, the maximum available on the analyzer.[2]

The general procedure followed was to determine which probe coupled best to the lower frequency modes of the TM_{11}-like band, using the signal generator. Because of the orientation of the probes in the test waveguide, the largest signal results from vertical rather than horizontal displacement of the beam. A data acquisition computer was used to read out the stripline monitors and produce a beam path display for both horizontal and vertical planes. The usual displacement was 0.25cm above and parallel to the axis. The beam pulse used was nominally 1.0A peak with a full width of 15ns. The linac repetition rate was 15Hz.

The Tektronix 492P spectrum analyzer used is equipped with preselection and digital storage options. The preselector was essential for reducing spurious responses to a manageable number. It did, however, require routine peaking. Digital storage, which included a "maximum hold" function, was used to accumulate spectra over several minutes, allowing fairly fine features to be resolved. Usually, the sweep was set at the lowest available rate (50 seconds across the screen) to minimize the space between the 15Hz repetition lines. Four or five sweeps were required to clean up the repetition lines. In addition to selecting 1 MHz bandwidth for reasons discussed above, we used the "pulse stretcher" function and defeated the video filters for maximum response to short pulses.

Results

Figure 4 shows the beam-induced power spectrum in the third cell of the SLAC type waveguide model. For comparison, the TM_{11}-like band power spectrum in the first cell, when the waveguide is excited in the third cell by the signal generator, appears in Fig. 5. Consistent with earlier reports from SLAC[1], the predominant excitation by the beam is in the lowest frequency mode. This turned out to be generally true for all four waveguide models.

Another characteristic of SLAC waveguide which appears to be generally true among our test models is that the strongest beam-induced HEM_{11} modes do not

0018-9499/85/1000-2329$01.00© 1985 IEEE

extend past the first ten or so cells. As an example, the cell excitation pattern for the unslotted contoured cavity model appears in Fig. 6.

We found that the energy imparted to the HEM_{11} mode by the beam is approximately proportional to the square of the component of beam offset along the polarization axis of the mode (Fig. 7). In attempting to minimize HEM_{11} excitation by steering the beam precisely along the axis of the waveguide, we found that 15 dB improvement over the excitation level seen with an offset of 4mm was about the best we could achieve. This implies a pulse-to-pulse beam centroid wander on the order of 0.7mm.

Excitation levels obtained with the nominal beam conditions described above are given in Table 1 for the strongest HEM_{11} modes. For very undercoupled probes, the stored energy in the mode is proportional to the observed power divided by the coupling coefficient. This quantity is given in the last column of Table 1. Given that the loaded quality factors of the modes are close to 13,000 for all the modes, and neglecting small differences in frequency, the P/β values of different modes and test waveguides can be compared, a lower valve indicating a weaker beam breakup interaction.

Acknowledgements

The authors wish to acknowledge the contributions of many people on the Boeing Radiation Effects Laboratory staff in preparing and executing these experiments, especially the machine shop staff, the accelerator operations group, and Dian Yeremian and Barry Robinson, who provided the stripline readout system.

References

1. R. H. Helm, G. A. Loew, "Beam Breakup", in Linear Accelerators, P. M. Lapostolle and A. L. Septier, ed., p. 173; North-Holland Publishing Company, Amsterdam (1970).

2. M. Engleson, Modern Spectrum Analyzer Theory and Applications, section 5.4, Artech House, Inc., Sedham, Massachusetts (1984).

TABLE 1

Test Waveguide			HEM_{11} Mode				
Cell Configuration	Phase Shift Per Cell	Typical Aperture (in)	Frequency (MHz)	Cell	Probe Power (dBm)	β (10^{-3})	P/β (μw)
Disk-Loaded	$2\pi/3$	1.0	4146	3	-36	14	18
			4154	3	-41	4.9	16
			4162	3	-44	1.4	28
Disk-Loaded	$3\pi/4$	1.0	4191	3	-43	.35	140
Contoured Cavity	$3\pi/4$	1.5	3948	3	-42	7.2	8.8
			3962	3	-42	21	3.0
			3983	3	-45	5.2	6.1
Contoured Cavity/ Slots	$3\pi/4$	1.5	4122	1	-53	3.8	1.3

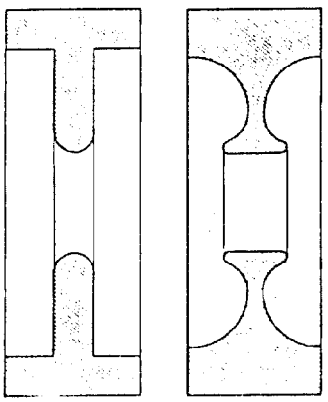

Figure 1. Longitudinal cross section of (a) disk-loaded and (b) Boeing contoured cavity waveguides.

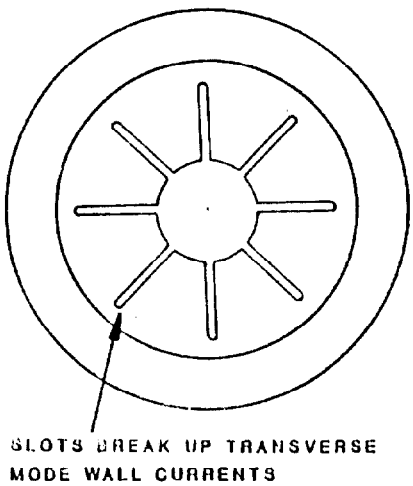

Figure 2. Radial iris slots in one of two contoured cavity waveguides.

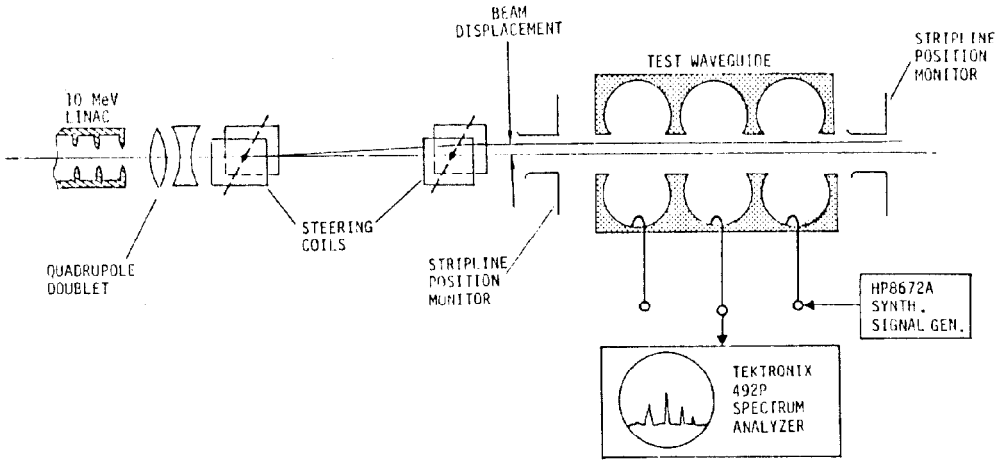

Figure 3. Schematic beamline layout for observation of beam-induced dipole modes.

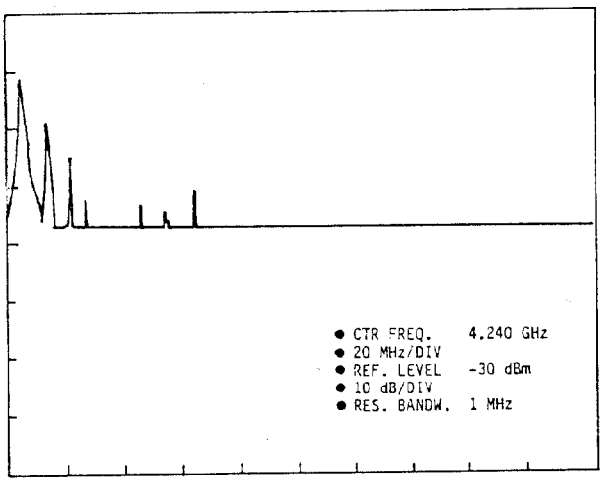

Figure 4. Sample beam-induced power spectrum seen in third cell of disk-loaded, $2\pi/3$ phase shift waveguide.

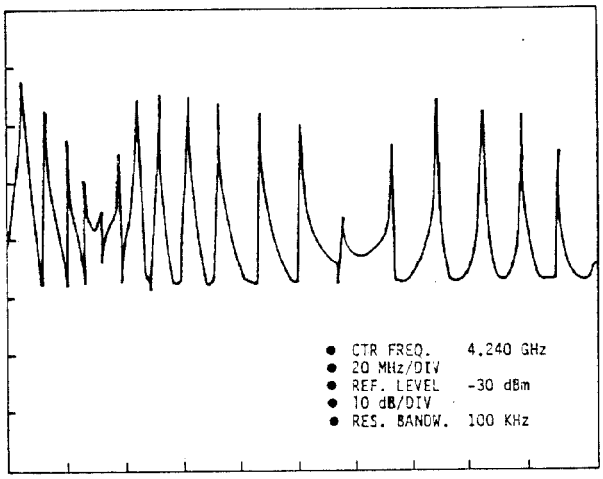

Figure 5. Dipole modes of the disk-loaded $2\pi/3$ phase shift waveguide. Signal is injected in third cell, monitored in first cell.

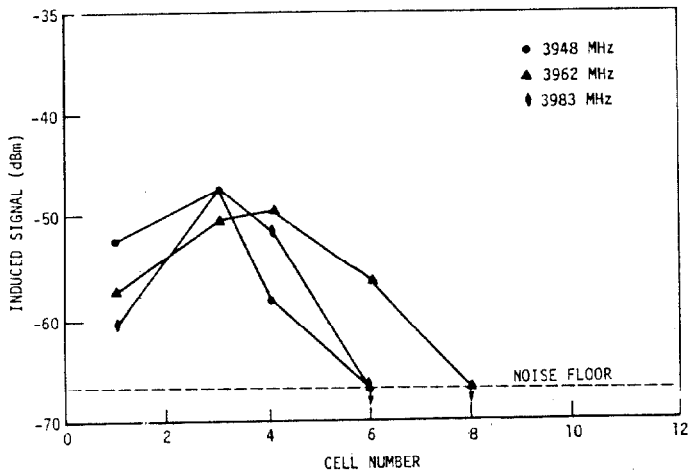

Figure 6. Cell excitation patterns for three strongest beam-induced modes in contoured cavity waveguide.

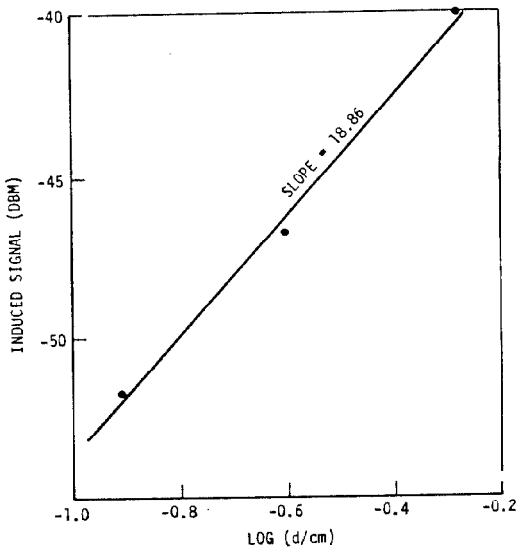

Figure 7. Dependence of 3948 MHz induced signal on beam offset d in contoured cavity waveguide. Least squares fit has a slope of 5.7dB per factor of two displacement.